Electronic structure of a two-dimensional Penrose lattice: Single- and two-component systems

F. Aguilera-Granja, F. Mejía-Lira, and J. L. Morán-López
Instituto de Física, Universidad Autónoma de San Luis Potosí, 78000 San Luis Potosí, San Luis Potosí, Mexico

R. G. Barrera*
Departamento de Física, Centro de Investigación y de Estudios Avanzados del Instituto Politécnico Nacional, Apartado Postal 14-740, 07000 México, Distrito Federal, Mexico

(Received 9 December 1986; revised manuscript received 20 May 1987)

The electronic structure of a two-dimensional Penrose lattice is calculated within the tight-binding Hamiltonian. By means of the cluster Bethe-lattice method, we study the dependence of the local density of states (LDS) on the cluster size for two different geometries. We find that very large clusters are necessary to obtain the main features of the LDS. The method is applied to a single-component system and to an ordered binary alloy.

I. INTRODUCTION

The experiments of Schechtman *et al.*[1] that showed the existence of quasicrystals opened a new field in solid-state physics. The characteristic of those systems is the presence of a new kind of order that is neither crystalline nor amorphous; i.e., the x-ray diffraction pattern of those samples shows icosahedral symmetry, incompatible with traditional crystallography.[2]

Several models have been proposed to explain the unexpected experimental results obtained from rapidly cooled $Al_{0.86}Mn_{0.14}$ alloys.[3] Among others, the three-dimensional extension of the Penrose lattice seems to be an acceptable model, which reproduces the observed crystallographic data.[4] A question that naturally arises is, what are the physical properties of this new kind of materials? Some answers on the electronic and vibrational spectra have been given in recent papers.[5–7] However, those properties are far from being fully understood and a more extensive study is still necessary.

The Penrose lattice is formed by two-dimensional tiles that cover the plane completely in a nonperiodic fashion.[8,9] A simple model of the quasicrystal consists in assuming that the atoms occupy the vertices of the tiles and that the electrons hop only through the edges. As a consequence of the lack of periodicity, it is not possible to obtain an exact solution of the electronic spectra and only numerical results can be obtained for finite clusters.

Here we study systematically, in the framework of the tight-binding Hamiltonian and within the cluster Bethe-lattice method[10] (CBLM), how the electronic local density of states (LDS) depends on the local geometry and on the cluster size. The reasons for using the Bethe lattice as a boundary condition are the following:[10] (i) the density of states of the Bethe lattice is smooth and featureless; consequently any structure found in the local density of states of any specific atom in a cluster Bethe-lattice system is very closely associated with the local environment of this atom; and (ii) the Bethe lattice allows us to close in an analytic way the coupled set of equations for the local Green's functions.

First, we consider systems with one component in two different geometries, and calculate the LDS at sites with different local environments. In general we find that, in contrast to the crystalline case, large clusters (~ 100 sites) are necessary to obtain the main characteristics of the LDS. In addition, we find that in one of the geometries a localized state appears at the center of the band, at the central atom, and in ten equivalent sites of coordination number three, in agreement with what has been reported previously[7] using symmetry arguments.

It is a characteristic of the Penrose lattice that it can be subdivided into two nonequivalent sublattices,[7] α and β, such that an electron in an α site hops only to β sites and vice versa. We have also investigated the electronic spectra of a binary alloy A_xB_y ($y=1-x$) that is completely ordered in those sublattices; i.e., the A atoms in α and the B atoms in β sites. In this case, we have chosen as a boundary condition for the Bethe lattice the virtual-crystal approximation (VCA). To our knowledge these are the first results published for the case of a binary alloy in the Penrose lattice.

The CBLM formalism as applied to the Penrose lattice is given in Sec. II, where we present the equations of motion for the local Green's function for both cases, the single-component system and the alloy. Our results are presented and discussed in Sec. III.

II. THE CLUSTER BETHE-LATTICE METHOD

The cluster Bethe-lattice method has been extensively applied to the study of the electronic,[11] magnetic,[12] and vibrational[13] properties of alloys and single-component systems. It is a real-space approach in which the local topology of a given cluster of atoms is taken exactly into account and the rest of the crystal is simulated by a Bethe lattice.

In this study, we have calculated the LDS at various sites in clusters of different sizes in a Penrose lattice. The calculation is based in the tight-binding Hamiltoni-

an, which, under the assumption that the hopping matrix elements (t) are the same between nearest neighbors and setting the zero of energy in the on-site energies, takes the form

$$H=-\sum_{i,j} t\,|i\rangle\langle j|\ . \tag{2.1}$$

We illustrate how to calculate the equations of motion for the local Green's function of the Penrose lattice by the following example. Let us refer to the cluster of 46 atoms shown in Fig. 1(a). From the Dyson equation one obtains the coupled set of equations:

$$\begin{aligned}
EG_{00}&=1-5tG_{10}\ ,\\
EG_{10}&=-tG_{00}-2tG_{20}\ ,\\
EG_{20}&=-2tG_{10}-2tG_{30}-tG_{40}\ ,\\
EG_{30}&=-2tG_{20}-2tG_{50}\ ,\\
EG_{40}&=-tG_{20}-2tG_{50}-2tG_{60}-2t\gamma G_{40}\ ,\\
EG_{50}&=-tG_{30}-tG_{40}-tG_{70}\ ,\\
EG_{60}&=-tG_{40}-tG_{70}-t\gamma G_{60}\ ,\\
EG_{70}&=-2tG_{50}-2tG_{60}-t\gamma G_{70}\ ,
\end{aligned} \tag{2.2}$$

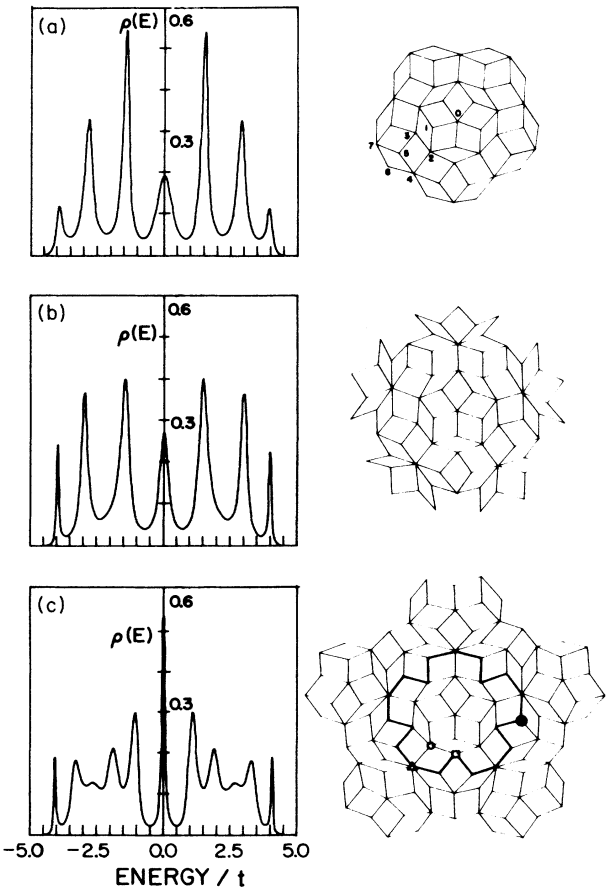

FIG. 1. Local density of states at the central atom of the clusters shown on the right-hand side. The energy is given in units of the hopping matrix element.

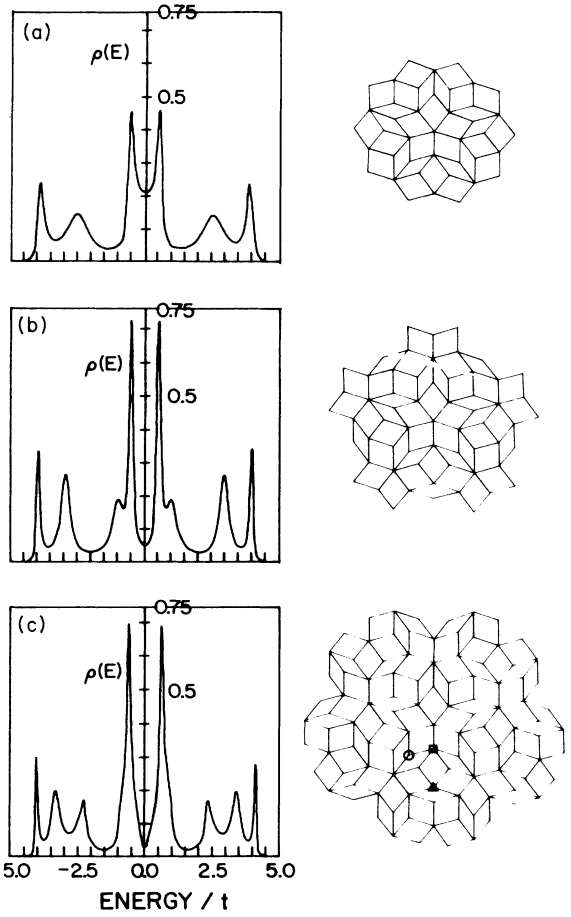

FIG. 2. Local density of states at the central atom of the clusters shown on the right-hand side. The energy is given in units of the hopping matrix element.

where we have closed the set of equations (2.2) assuming a Bethe lattice of coordination number z outside the cluster, and the transfer function γ is given by

$$\gamma=\{-E+[E^2-4(z-1)]^{1/2}\}/2(z-1)\ . \tag{2.3}$$

The average coordination number in the Penrose lattice

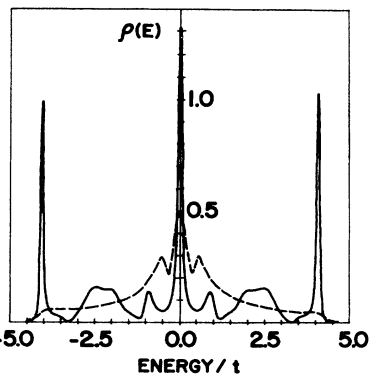

FIG. 3. Local density of states at the site marked with a solid circle, calculated in the CBLM (solid curve) and within the recursion method (Ref. 5).

is ~ 4.8; however, some states at the edges of the band are lost when the cluster is saturated with a Bethe lattice with that coordination number. In order to avoid this problem we took a larger coordination number (5.5), which is already enough to satisfy the normalization condition. Once the local Green's function is known, the LDS can be calculated from

$$\rho_0(E) = -\mathrm{Im}G_{00}(E)/\pi \ . \tag{2.4}$$

All the densities of states shown in Figs. 1–6 were calculated in a similar way.

We consider now the case of a binary alloy A_xB_y, with a Hamiltonian of the form

$$H = \sum_i \varepsilon_i \, | \, i \rangle \langle i \, | - \sum_{i,j} t \, | \, i \rangle \langle j \, | \ , \tag{2.5}$$

where the energies ε_i take values 0 (δ) if the atom under consideration is A (B) and where for simplicity we ignore off-diagonal disorder.

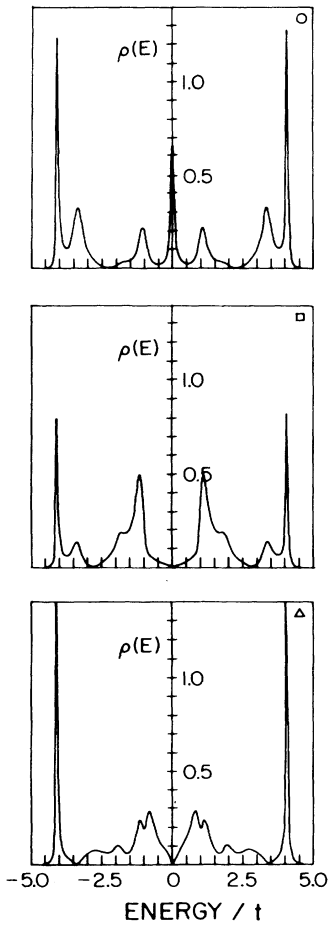

FIG. 4. Local density of states at the sites marked with a circle, a square, and a triangle in Fig. 1.

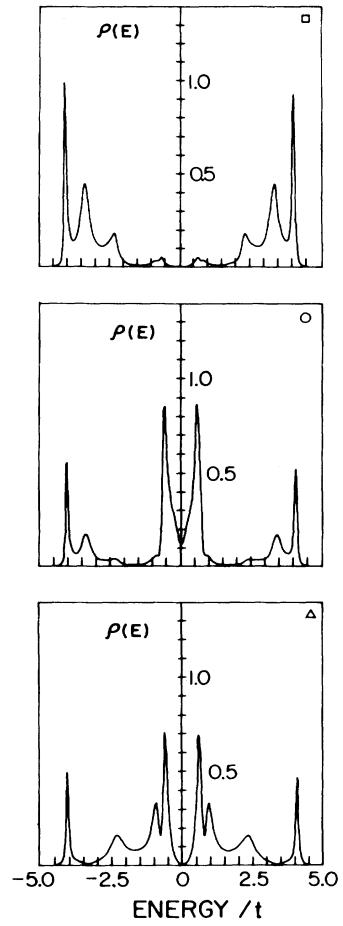

FIG. 5. Local density of states at the sites marked with a square, a circle, and a triangle in Fig. 2.

We considered only the case with the highest spatial order, i.e., where all nearest neighbors of a given atom are of the opposite kind. The cluster is shown in Fig. 7 and corresponds to an $A_{0.43}B_{0.57}$ alloy. The equations of motion in the case where the central atom is of type A are

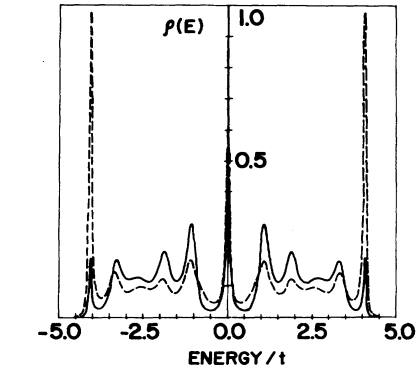

FIG. 6. Average density of states of the 31-atom subcluster of the 111-atom cluster shown in Fig. 1(c) (solid curve) and the LDS of the central atom of the same cluster (dashed line).

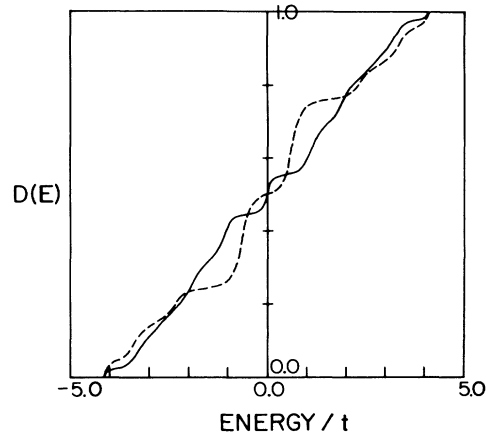

FIG. 7. Penrose lattice showing the ordered binary alloy whose electronic structure was calculated.

$$
\begin{aligned}
&EG_{00}=1-5tG_{10}\ ,\\
&(E-\delta)G_{10}=-tG_{00}-2tG_{20}-2tG_{30}\ ,\\
&EG_{20}=-2tG_{10}-tG_{30}\ ,\\
&EG_{30}=-tG_{10}-tG_{40}-tG_{50}\ ,\\
&(E-\delta)G_{40}=-tG_{20}-2tG_{30}-2tG_{60}-tG_{70}\ ,\\
&\vdots
\end{aligned}
\tag{2.6}
$$

We embedded the alloy cluster in a medium with an average on-site energy (virtual-crystal approximation) $\varepsilon=x\varepsilon_A+y\varepsilon_B$.

III. RESULTS AND DISCUSSION

We considered two types of geometries (we call them types I and II), constructed with thick and thin rhombuses, with sides of equal length. As a first approximation, we assume that the hopping integrals in the tight-binding Hamiltonian are the same for the whole system. A more accurate calculation should consider the various local atomic environments characteristic of the Penrose lattice.

Figures 1 and 2 contain the LDS at the central site of the various clusters considered and shown on the right-hand side. The number of sites taken into account exactly in clusters *a*, *b*, and *c* of geometry I are 46, 71, and 111, respectively. The main characteristic of the LDS is the central peak that grows as the number of sites is increased. Simultaneously, the density of states at the nearest minimum decreases. Extrapolations of numerical calculations[7] indicate that the state at $E=0$ is strictly localized with a weight of 0.09 ± 0.01 in the middle of a gap with limits $E_0=\pm0.163\pm0.007$. It is clear that in order to obtain those properties, clusters much larger than those considered here are necessary. However, the main trends are already present in our results. For example, the integration of the number of states in the central peak in the largest cluster (111 atoms) already yields 0.1.

Very different results are obtained for the geometry of type II. In this case a minimum in the density of states is obtained at $E=0$, leading probably to a gap for infinite clusters. The number of atoms in the clusters considered here are 41, 61, and 106, respectively. A comment that applies to all the densities of states calculated in the CBLM is that the high peaks that appear at the edges of the band do not have any physical significance. They are produced by the interface between the cluster and the Bethe lattice and in general get smaller as the size of the cluster is increased.

We also calculated the LDS at noncentral sites. Figure 3 contains the results for the LDS at the three-coordinated site marked by a solid circle in Fig. 1(c) (solid line). The LDS at the same site (dashed line), calculated by the recursion method for 200 levels,[5] that corresponds to a system of approximately 3000 atoms, is also shown for comparison. One observes that the central peak and the two shoulders are already present in our calculation.

Figures 4 and 5 contain the LDS calculated at the sites marked with a square, an open circle, and a triangle in Figs. 1(c) and 2(c). These results clearly show the dependence on the local topology. It is worth noticing that the peaks at the edges of the band get higher, the nearer the atom under consideration is to the boundary.

We calculated the LDS at all the sites of the subcluster marked with the thick line in the cluster shown in 1(c). The average LDS obtained from the 31-atom subcluster is shown in Fig. 6 and compared with the LDS obtained for the central atom. One observes that the central part of the two LDS's is very similar and that the main difference is at the edges, due to the boundary effects mentioned above.

In Fig. 8 we plot the integrated density of states $D(E)$ as a function of energy for the central atom in the clus-

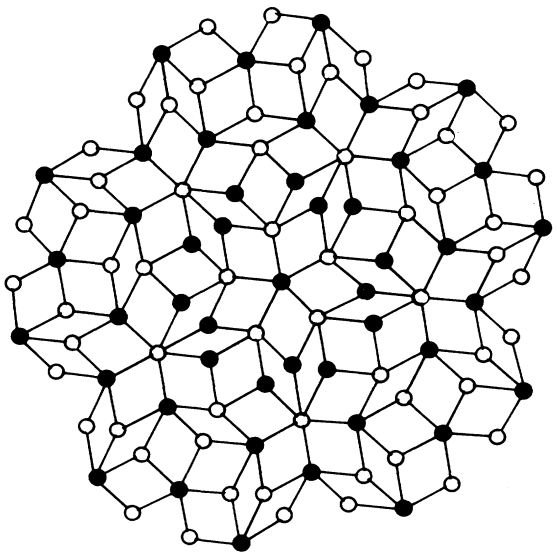

FIG. 8. Integrated density of states as a function of energy at the central atoms of the clusters shown in Fig. 1(c) (solid curve) and 2(c) (dashed curve).

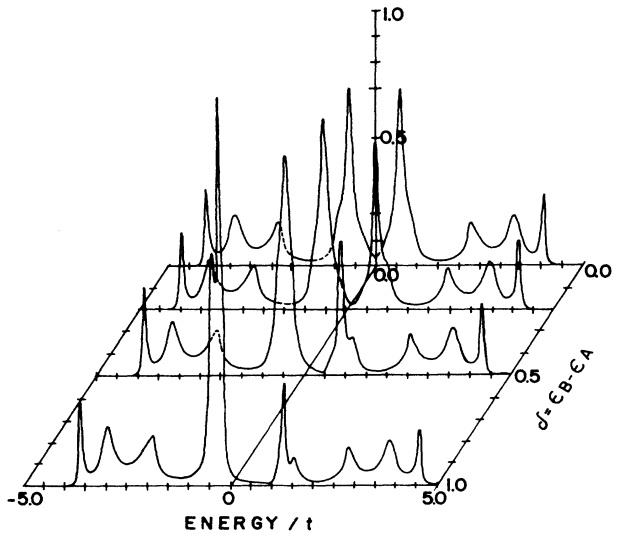

FIG. 9. Local density of states at the central atom (A) of the Penrose binary alloy shown in Fig. 7, for several values of the diagonal disorder $\delta=\varepsilon_B-\varepsilon_A$.

ters shown in Figs. 1(c) and 2(c). The solid (dashed) curve corresponds to the geometry of type I (II). One sees in the solid line a central step that is expected[7] to become steeper as the cluster size increases, due to the presence of the localized state mentioned above.

The results for the LDS at the central site in the ordered binary alloy $A_{0.43}B_{0.57}$ with geometry of type II are shown in Fig. 9. It corresponds to the most ordered array, where each A (B) atom is surrounded by B (A) atoms. The third coordinate is the difference in the on-site energies $\varepsilon_B-\varepsilon_A=\delta$. One sees that the consequence of the spatial order is to stress the tendency to form a gap between the values of ε_i. In the case of interpenetrating sublattices with an equal number of sites, a gap appears due to the additional symmetry of the system. One also observes small modifications in the peaks near the gap region with an increment of the number of states in the low-energy region ($E<\varepsilon_A$).

Due to the inequivalency of the sublattices, we decided to close the set of equations with an average alloy, whose on-site potential is given by the virtual-crystal approximation. The VCA is the crudest approximation to the alloy potential which simply scales the position of the energy band linearly with the concentration of each species. This is a good approximation only if the difference δ is small compared with the constituent bandwidths. A better choice in the boundary conditions may result in a more evident gap and may give rise to additional localized states.[14]

As a general conclusion one might say that the main features of the electronic spectra in a Penrose lattice can be obtained by means of the CBLM. However, in this case the size of the cluster necessary to obtain equivalent results to the corresponding ones in crystalline lattices is much larger. Due to the simplicity of the method, it might be especially useful for the case of an alloy where additional localized states might appear due to the substitutional disorder.

ACKNOWLEDGMENTS

This work was partially supported by the Dirección General de Investigación Científica y Superación Académica de la Secretaría de Educación Pública, México, Distrito Federal, Mexico, under Contracts No. 86-01-285 and No. 86-01-294, by Programa Regional de Desarrollo Científico y Tecnológico de la Organización de Estados Americanos, and by Consejo Nacional de Ciencia y Tecnología (CONACyT), México, Mexico, under Contract No. PCEXCNA-040428.

*On leave from Instituto de Física, Universidad Nacional Autónoma de México, Apartado 20-364, 01000 México 20, Distrito Federal, Mexico.

[1]D. S. Schechtman, I. Blech, D. Gratias, and J. W. Cahn, Phys. Rev. Lett. **53**, 1951 (1984).
[2]P. A. Bencel, P. A. Heiney, P. W. Stephens, A. I. Goldman, and P. M. Horn, Phys. Rev. Lett. **54**, 2432 (1985).
[3]D. R. Nelson and B. I. Halperin, Science **229**, 233 (1985).
[4]A. L. Mackay, Physica **114A**, 609 (1982).
[5]T. C. Choy, Phys. Rev. Lett. **55**, 2915 (1985).
[6]T. Odagaki and D. Nguyen, Phys. Rev. B **33**, 2184 (1986); V. Kumar and G. Athithan, *ibid.* **35**, 906 (1987).
[7]M. Kohmoto and B. Sutherland, Phys. Rev. Lett. **56**, 2740 (1986).
[8]R. Penrose, Bull. Inst. Math. Appl. **10**, 266 (1974).
[9]M. Gardner, Sci. Am. **236** (January), 110 (1977).
[10]J. D. Joannopoulos and F. Yndurain, Phys. Rev. B **10**, 5136 (1974).
[11]R. C. Kittler and L. M. Falicov, Phys. Rev. B **18**, 2506 (1978).
[12]J. B. Salzberg, C. E. T. Gonçalves da Silva, and L. M. Falicov, Phys. Rev. B **14**, 1314 (1976).
[13]R. A. Barrio, F. L. Galeener, and E. Martínez, Phys. Rev. Lett. **52**, 1786 (1984).
[14]S. Kirkpatrick and T. P. Eggarter, Phys. Rev. B **6**, 3598 (1972).